Functional connectivity in the prefrontal cortex measured by near-infrared spectroscopy during ultrarapid object recognition

Andrei V. Medvedev,[a] Jana M. Kainerstorfer,[a,b,*] Sergey V. Borisov,[a,†] and John VanMeter[a]
[a]Georgetown University Medical Center, Center for Functional and Molecular Imaging, Washington, DC
[b]University of Vienna, Department of Physics, Vienna, Austria

Abstract. Near-infrared spectroscopy (NIRS) is a developing technology for low-cost noninvasive functional brain imaging. With multichannel optical instruments, it becomes possible to measure not only local changes in hemoglobin concentrations but also temporal correlations of those changes in different brain regions which gives an optical analog of functional connectivity traditionally measured by fMRI. We recorded hemodynamic activity during the Go-NoGo task from 11 right-handed subjects with probes placed bilaterally over prefrontal areas. Subjects were detecting animals as targets in natural scenes pressing a mouse button. Data were low-pass filtered <1 Hz and cardiac/respiration/superficial layers artifacts were removed using Independent Component Analysis. Fisher's transformed correlations of poststimulus responses (30 s) were averaged over groups of channels unilaterally in each hemisphere (intrahemispheric connectivity) and the corresponding channels between hemispheres (interhemispheric connectivity). The hemodynamic response showed task-related activation (an increase/decrease in oxygenated/deoxygenated hemoglobin, respectively) greater in the right versus left hemisphere. Intra- and interhemispheric functional connectivity was also significantly stronger during the task compared to baseline. Functional connectivity between the inferior and the middle frontal regions was significantly stronger in the right hemisphere. Our results demonstrate that optical methods can be used to detect transient changes in functional connectivity during rapid cognitive processes. [DOI: 10.1117/1.3533266]

Keywords: near-infrared spectroscopy; brain hemodynamics; functional connectivity; independent component analysis; object detection; prefrontal cortex.

Paper 10052SSR received Feb. 1, 2010; revised manuscript received Sep. 8, 2010; accepted for publication Nov. 19, 2010; published online Jan. 28, 2011.

1 Introduction

Near-infrared spectroscopy (NIRS) is a developing technology for low-cost noninvasive brain imaging with a growing use in research and clinical practice. Traditionally, it is used to measure local changes in hemoglobin concentrations and spatial image reconstruction (diffuse optical tomography). NIRS is a novel imaging technique with several unique features whose capabilities have not yet been fully explored. Developed over the past 20 years mainly to measure changes in regional blood oxygenation and flow caused by neuronal activity, it detects hemodynamic modulation as an indirect measure of neuronal activity. NIRS is a promising tool because it can potentially provide an imaging method with reasonable spatial and excellent temporal resolution [as found in electrophysiological methods such as electroencephalography (EEG) and magnetoencephalography (MEG)] complementary to other imaging methods based on the hemodynamic response [functional magnetic resonance imaging (fMRI) and positron emission tomography, (PET)]. With multichannel optical instruments, it also becomes possible to measure not only local changes in brain areas independently from each other but also temporal correlations of those changes, therefore deriving an NIRS-based "functional connectivity" similar to the that measured by the fMRI BOLD signal.[1]

In the present study, we have explored the feasibility of using NIRS technology to image activation and functional connectivity in the prefrontal cortex of healthy subjects during a rapid object recognition task (target detection). Such tasks are commonly used to study the mechanisms of selective attention, which plays an important role in goal-directed behavior. As has been shown in many studies using electrophysiological techniques, the process of recognition of complex (but familiar) objects is very rapid. For example, Thorpe et al.[2] have used a Go-NoGo task for rapid detection of animals in complex natural scenes presented for 30 ms. A response was required from subjects when a target (animal) was detected (the "Go" condition) and a response was otherwise withheld (the "NoGo" condition). It has been shown that target and nontarget event-related potentials (ERPs) start to diverge from each other at ~150 ms, reaching a peak at 200 ms, and the reaction time is usually within 350–450 ms after presentation of the stimulus.[2] The so-called differential ERP activity (the difference between target- and nontarget-related ERPs) has negative polarity over temporal-occipital cortices and a positive polarity over the frontal cortex. The Go-NoGo task has been also used as a binary task (requiring either producing or

*Current address: Section on Analytical and Functional Biophotonics, PPITS, NICHD, National Institutes of Health, Bethesda, Maryland 20892.
†Current address: Goethe University, Department of Neurology and Brain Imaging Center, Frankfurt, Germany.

Address all correspondence to: Andrei V. Medvedev, CFMI, GUMC, Preclinical Science Building, LM 14, 3900 Reservoir Road NW, Washington, DC 20057. Tel: 202–687-5126; E-mail: am236@georgetown.edu.

1083-3668/2011/16(1)/016008/10/$25.00 © 2011 SPIE

withholding a behavioral response) in various contexts to discriminate between sensory stimuli of different modalities.[3] The initial interpretation of the involvement of frontal regions in the Go-NoGo tasks was that frontal activity reflects inhibition of the behavioral response during detection of nontarget stimuli.[2,3] However, in the context of discrimination of complex visual objects this interpretation seems to be insufficient[4] because of the dependence of the frontal response on stimulus properties.[5–9] It has been suggested that early ERP components at 150–250 ms during complex object discrimination task may be related to higher-level categorization processes,[10] however, this suggestion needs further experimental confirmation.

Little is known about anatomical localization and hemispheric lateralization of the sources of the early differential ERP activity in the visual discrimination Go-NoGo tasks. A more recent study from Thorpe's group revealed bilateral generators in the temporal-occipital regions,[11] suggesting those generators being a part of the visual ventral processing stream. Because of insufficient spatial sampling in many EEG instruments, only a few studies have attempted to perform anatomical localization of sources of the early posterior-anterior differential ERPs. Using ERP source localization techniques, Codispoti et al.[4] have found sources of activity related to the object detection task within the posterior visual-associative brain regions and, although less pronounced, additional anterior sources in the prefrontal cortex, which were slightly more pronounced in the right versus left hemisphere at $t = 175$–200 ms.

In the present study, we have used optical imaging of the prefrontal cortex in combination with high-density EEG (128 channels) to further study the spatial and temporal aspects of the involvement of the prefrontal cortex in the visual complex object discrimination task. In this report, we present preliminary data with the major goal to assess the applicability of noninvasive optical imaging as a tool for hemispheric lateralization of cognitive tasks. Specifically, we measured not only the amplitude of optical responses with subsequent reconstruction of spatial maps of functional activation but also a correlation of signals within the investigated areas to study local and bilateral functional connectivity during task performance.

2 Methods

2.1 *Participants*

Eleven right-handed young adults (five females, age 18–30, mean age 23) participated in the study. All participants signed a consent form approved by the Georgetown University Institutional Review Board and reported as being in good health and without medications. All subjects had normal (or corrected-to-normal) vision and undertook a battery of behavioral tests that included measures of IQ (Weschler Abbreviated Scale of Intelligence; the average IQ score 121.7) and handedness before one experimental session lasting 2 h, during which they performed a target-detection task with simultaneous optical and EEG recording of brain activity. All subjects were compensated for their participation in these experiments.

2.2 *Optical Data Collection*

Optical signals were recorded using a continuous-wave CW5 imaging system (TechEn, Inc., Milford, Massachusetts) that measures the amplitude of light traveling through the brain and surrounding tissue. The CW5 system has 32 frequency-division multiplexed sources emitting light at two wavelengths, 690 and 830 nm (i.e., 16 lasers at each wavelength), and 32 detector channels. Continuous parallel operation of all the sources and detectors allows rapid data collection. Each laser is modulated at a different frequency from 6.4 to 12.8 kHz, with intervals of 200 Hz between adjacent lasers to allow subsequent frequency demodulation and separation of individual source-detector pairs. Each detector is based on a Hamamatsu APD module (C5460–01) followed by signal amplification and collects light from all sources simultaneously. All optical signals are initially sampled at 41.7 kHz, using four NI6052E data acquisition cards (National Instruments Corporation, Austin, Texas). After the detected signals have been digitized and saved to disk, they are demodulated in software to determine the contribution at the detector from each source.

2.2.1 *Optical probes*

The light sources and detectors of the CW5 instrument were connected to the subject's head by flexible optical fiber bundles. Their front ends (optodes) were arranged on a supporting plastic base in a geometrical configuration to allow detectors to "see" as many neighboring sources as possible (source-detector separation was 3 cm). For the specific goals of the current project, we used an optical probe that could be put on top of the 128-electrode net manufactured by Electrical Geodesic, Inc. [(EGI), Eugene, Oregon]. This allowed us to record optical and EEG signals simultaneously. Two 14×8-cm probes, each accommodating 11 optodes with three dual-wavelength (690 and 830 nm) laser sources and eight optical detectors for each hemisphere, were placed bilaterally using anatomical landmarks of the international 10–20 EEG system and aiming to cover the area between locations F3/4-F7/8-C3/4, that is, the inferior frontal gyrus (IFG) and the middle frontal gyrus (MFG) (Fig. 1).

2.3 *Experimental Paradigms*

The paradigm used in this study was based on the Animal-No Animal Go-NoGo task introduced by Thorpe et al.[2] to study fast object recognition using the ERP technique. In this paradigm, we used black-and-white pictures of natural scenes (size of 472×728 pixels), which were normalized in terms of brightness and contrast. Pictures were presented to the subjects for 26 ms at the center of a computer LCD monitor at a viewing distance of 75 cm and an angular size of 10 deg in 12 blocks, each containing 100 pictures. The intertrial interval within each block varied from 900 to 1700 ms, and there were 20-s breaks between successive blocks. Thus, 1200 pictures selected randomly from the same picture set were presented in each experiment. Approximately 50% of pictures contained animals (targets) and pictures without animals served as nontargets. The task was to simultaneously press two buttons on a button box in response to pictures containing targets as quickly as possible using the thumbs of both hands. During all interstimulus intervals, a crosshair was present in the middle of the screen and subjects were asked to permanently focus their gaze on this cross thus minimizing eye movements. Each experiment was preceded by a 2-min recording period in the state of quiescence, when subjects

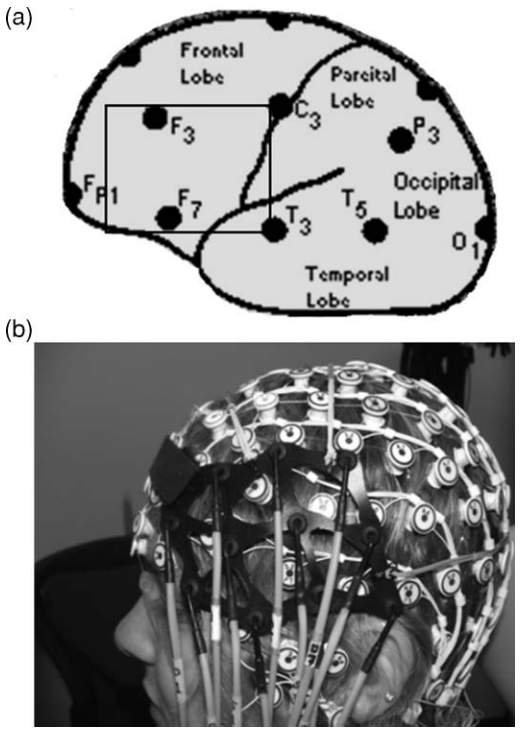

Fig. 1 (a) Position of the left optical probe in reference to the locations of the 10–20 EEG electrode placement system. The right probe was placed symmetrically on the right side of the head. (b) Combined optical and EEG recording probe.

were sitting passively with their eyes open and looking at the crosshair in the center of the monitor (for 1 min) and then eyes closed for another minute. These periods of passive wakefulness were used to assess the baseline level of functional connectivity.

2.4 *Optical Data Analysis*

After offline frequency demodulation, optical data were filtered <1 Hz, downsampled to 20 samples per second, and stored on an acquisition PC computer for further analysis. Independent component analysis (ICA) was performed, and artifactual components generated by superficial layers (scalp and skull) as well as cardiac and respiratory signals were removed using the approach as described previously.[12]

After the ICA procedure, optical signals from 1 s before and up to 30 s after the beginning of each block with picture presentations were used to calculate relative changes in concentration of oxygenated (HbO) and deoxygenated (Hb) hemoglobin using the open-source software HOMer (Photon Migration Laboratory, Massachusetts General Hospital, Charlestown, Massachusetts; http://www.nmr.mgh.harvard.edu/PMI/resources/homer/home.htm). Two-dimensional images of those changes were also reconstructed for each subject using the back-projection algorithm implemented in the HOMer package, which approximates the convexity of the scalp by flat surface and uses semi-infinite homogenous slab geometries. Thus, a resulting two-dimensional scalp map does not depend on an individual "realistic" head space and is based only on the flat-probe geometry, which may be considered as an anatomical template. This facilitates cross-subject averaging and group-level analysis because the individual data are automatically warped into the standard (flat) probe and then simply averaged across subjects. Scalp maps were created using $14\times8 = 112$ voxels (1×1 cm each) within a rectangular covering each (left or right) probe [Fig. 2(a)]. Hemodynamic activity reconstructed for each voxel and each time point (thus giving its time course) is referred to as an optical channel.

At the beginning of an experiment, head measurements were taken and the standard locations Cz, C3, F3, F7, and T3 in the left hemisphere (and the corresponding locations in the right hemisphere) from the international 10–20 system for the placement of EEG electrodes were determined for each individual subject. Then, a 128-channel EGI electrode sensor net was placed on the subject's head and the placement of the corresponding electrodes at the 10–20 locations was verified. Optical probes were positioned on top of the electrode net using electrodes C3/4, F3/4, F7/8, and T3/4 as reference points [Figs. 1 and 2(a)]. Thus, the left probe was positioned to have (*i*) electrode F7 between source 1 and detectors 2 and 4, (*ii*) electrode F3 between detectors 3 and 5, and (*iii*) electrode T3 just behind detector 8 [Fig. 2(a)]. Similarly, the right probe was placed using electrodes F8, F4, and T4 as a coordinate system. A conventional conceptual knowledge about the exact locality

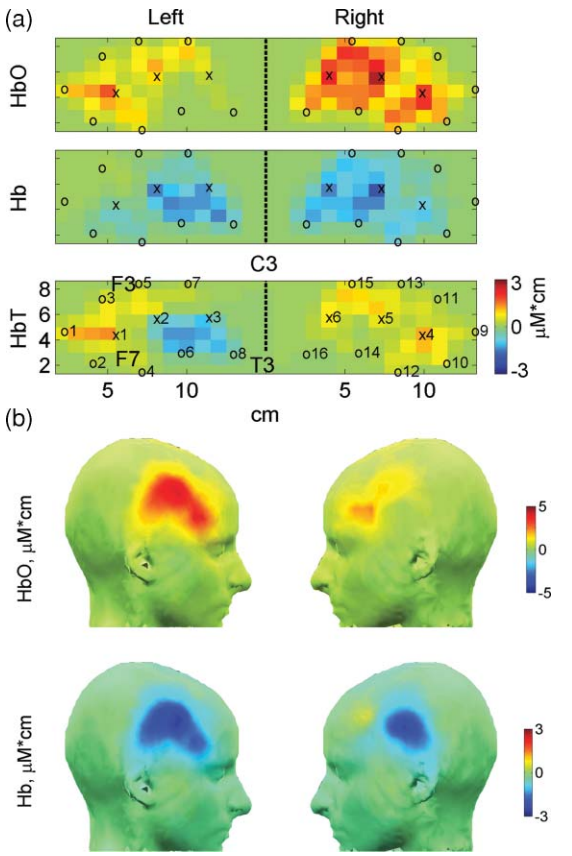

Fig. 2 Scalp maps of the group average hemodynamic amplitude responses shown in Fig. 8. (a) Two-dimensional maps reconstructed within the Homer software; positions of sources (x) and detectors (o) are shown as well as positions of anatomical marks F3, F7, T3, and C3 from the 10–20 electrode coordinate system, which were used to place the optical probe at the approximately same location in every subject. (b) The same maps as in (a) interpolated and projected on the surface of the head template using the EEGLAB software.

of the 10–20 electrodes has been confirmed in a recent study.[13] Specifically, F3/F4 electrodes have been shown to be located on left/right middle frontal gyrus, between posterior 1/3 and 1/2; whereas F7/F8 electrodes are located on pars triangularis of left/right inferior frontal gyrus.[13] Taking this information into account, we assumed that source-detector pairs from the lower half of the left probe (i.e., s1-d2, s1-d4, s1-d6, s2-d4, s2-d6, s3-d6, s3-d8) reflect the activity of the left IFG, whereas source-detector pairs from the upper half (i.e., s1-d1, s1-d3, s1-d5, s2-d3, s3-d5, s2-d7, s3-d7) reflect the activity of the left MFG [Fig. 2(a)]. Accordingly, the corresponding source-detector pairs from the lower/upper halves of the right probe were taken as reflecting the activities of the right IFG/MFG, respectively.

As an analog of functional connectivity based on correlation of the fMRI BOLD signals,[1] we calculated coefficients of correlation between the time courses of activities of all optical channels (that is, voxels) using the "corrcoef" Matlab function (The Mathworks Inc., Natick, Massachusetts) and used those correlations as measures of functional connectivity. Coefficients of correlation (here referred to as correlations) were calculated separately for oxy- and deoxygenated hemoglobin thus giving two separate measures of connectivity. Using original Matlab scripts, we calculated pairwise correlations between all optical channels in each subject and divided them into the following four groups: 1 and 2–unilateral correlations [all pairwise correlations between channels within the IFG and channels within the MFG, separately for the left (1) and the right (2) hemispheres]; and 3 and 4–bilateral correlations [between all homologous channels within the left/right IFG (3) and the left/right MFG (4)].

2.5 *Statistical Analysis*

Changes in concentration (here referred to as "amplitudes of the hemodynamic response") relative to the 1-s baseline periods before the beginning of each block were averaged over the first 30-s intervals within each block and either over all channels in each hemisphere or separately for the IFG and the MFG in the left and the right hemispheres. These values were analyzed by a two-way ANOVA test ($p < 0.05$) with regions of interest (left and right IFG, left and right MFG) as fixed effects and subjects as random effects. All correlations were subjected to Fisher's z-transform (making their statistical distributions close to normal distributions), and z-correlations during cognitive task (condition 3) were compared to z-correlations during baseline periods with eyes closed (condition 1) and eyes open (condition 2). These comparisons were made through a two-way ANOVA test ($p < 0.05$) with functional states (eyes closed, eyes open, or cognitive task) as fixed effects and subjects as random effects. In all cases, pairwise statistical comparisons were made with correction for multiple comparisons based on Dunn–Sidak's approach.[14]

2.6 *EEG Data Analysis*

The standard preprocessing procedure for EEG included filtering (bandpass 1–100 Hz), artifact detection and removal, segmentation, and baseline correction. EEG data were also subjected to ICA, which allowed us to identify artifacts related to eye blinks and eye movements, motion-related as well as physiological artifacts (mostly heartbeat related). All these artifacts were removed during restoration of the EEG signal from the corresponding ICA components with artifactual components excluded. Segmentation was done using epochs from –200 ms before (baseline period) and up to 800 ms after stimulus presentation. Target- and nontarget-related signals for each subject were averaged over 10 groups of trials (each group containing ~60 target- and ~60 nontarget-related trials) resulting in 10 sample ERPs for each subject. These sample ERPs were then subjected to time-frequency decomposition through deconvolution with Mortlet wavelets as implemented in the Fieldtrip software.[15] Such ERP-based time-frequency analysis preserves the phase-locked signal, and the resulting spectrograms are usually referred to as spectrograms of phase-locked or *evoked* oscillatory activity as opposed to the time-locked or *induced* oscillations when time-frequency decomposition is done on each trial first and then averaged.[16] Statistical analysis for EEG data was done using nonparametric permutation tests using the false discovery rate to account for multiple comparisons as implemented within the Fieldtrip software using the algorithm by Genovese et al.[17]

2.7 *Scalp Maps of Hemodynamic Response (Amplitude and Connectivity) and EEG*

To qualitatively represent changes in connectivity at the sublobar level (that is, between MFG and IFG within the same hemisphere, which we refer to as "unilateral connectivity"), for each voxel within the MFG we calculated its average correlation over all voxels within the IFG, and for each voxel in the IFG, we calculated its average correlation over all voxels within the MFG. These average correlations associated with each voxel (instead of pairs of voxels) could be mapped on a scalp map similar to the amplitude maps. To produce amplitude and correlation scalp maps, we used the normalized head template incorporated in the open-source EEGLAB software.[18] Specifically, the time courses of hemodynamic responses of all voxels (either amplitude or average correlation) were exported into the EEGLAB as multivariate time series analogous to the EEG along with spatial coordinates of the corresponding voxels determined in reference to the standard 10–20 electrode system as described earlier [see also Fig. 2(a)]. Function headplot within the EEGLAB package was used to create scalp maps shown in Fig. 2(b) (for hemodynamic amplitudes) and Fig. 3(b) (for hemodynamic correlations). For example, the map on Fig. 2(b) is a projection of the two-dimensional map shown in Fig. 2(a) onto the surface of the normalized scalp template (with interpolation causing a smoothing effect). Similarly, scalp maps of frequency components within the high β–low γ range (20–40 Hz) were produced for EEG responses (Fig. 4).

3 Results

3.1 *Independent Component Analysis of Optical Data and Removal of Systemic Artifacts*

The procedure for removal of systemic artifacts from optical data using ICA is illustrated by two examples in Figs. 5 and 6. It is well known that the most prominent physiological artifact contaminating optical signals is a cardiac signal reflecting

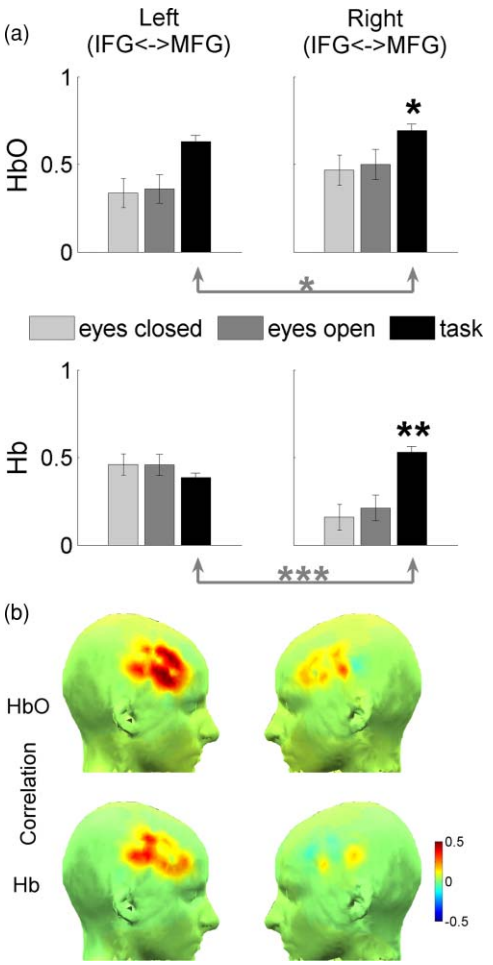

Fig. 3 Changes in unilateral (intrahemispheric) functional connectivity during the task. (a) Group average correlations between HbO signals and Hb signals averaged over the corresponding groups of channels/voxels pairwise during baseline periods (with eyes closed and open) as well as during the cognitive task. IFG and MFG are the inferior and the middle frontal gyrus, respectively. Significant changes are indicated by black asterisks (compared to baseline) and gray asterisks (left versus right hemispheres); $p < 0.05$ (*), $p < 0.01$ (**), and $p < 0.001$ (***). (b) Unilateral "connectivity maps" averaged over all subjects (see text for explanation how connectivity maps were created).

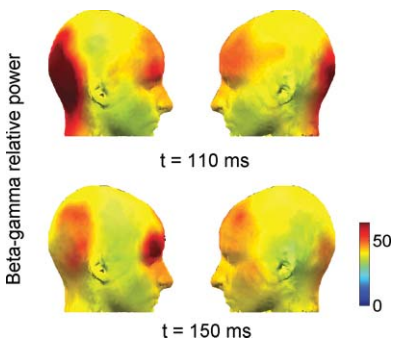

Fig. 4 Group average differential (targets > nontargets) scalp maps of high frequency activity 20–40 Hz) at times of earliest significant differences between targets and nontargets. Only pixels with significant values are shown ($p < 0.05$ corrected). Note the earliest activation at high frequencies 20–40 Hz in the occipital and prefrontal cortices ($t = 110$ ms) as well as the right hemispheric dominance of the response at β–γ frequencies especially evident at $t = 150$ ms when the response was at its maximum.

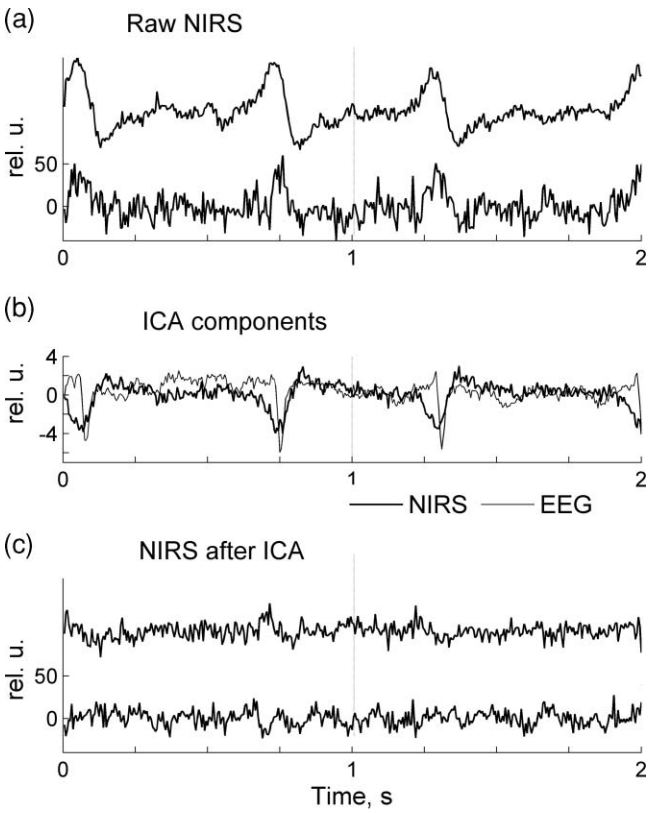

Fig. 5 (a) Raw optical signals are heavily contaminated by systemic physiological (cardiac) artifact. (b) Two independent components are shown that contain the cardiac artifact in the optical signal (thick line) as well as EEG (thin line). Those components have been removed during restoration of optical and EEG signals. (c) The same optical data as in (a) are shown after the removal of the cardiac artifact.

systemic transient changes in blood oxygenation with every heartbeat. In Fig. 5(a), two consecutive one-second epochs of raw data sampled at 200 Hz are shown for two channels recorded from subject 8. Both optical channels are heavily contaminated with cardiac artifact seen as high amplitude slow waves at frequency ~1.4 Hz. ICA was independently applied to NIRS and EEG data, and the components containing mostly the cardiac signal were identified for both NIRS and EEG [Fig. 5(b)]. The same optical channels shown in Fig. 5(c) after the removal of cardiac components are artifact-free and this demonstrates the effectiveness of ICA as a cardiac artifact-removing tool.

The next example illustrates the removal of the contribution of superficial layers from optical data. A representative 150-s segment with nine channels of raw optical data from subject 1 is shown in Fig. 6(a), and the corresponding power spectra are shown in Fig. 6(b). Because of low-pass filtering at 1 Hz and the removal of cardiac independent components, the most prominent physiological artifact in the optical data related to cardiac pulsation has been already removed. The remaining slow oscillations in the signal represent Mayer's waves (~0.1 Hz) related to autoregulation of vascular processes as well as respiratory pulsations identifiable as small spectral peaks at ~0.25 Hz [see channels 1, 5, 7, 8, 9 in Fig. 6(b)]. After ICA decomposition of the raw data, artifactual components related to the activity of superficial layers were identified as described earlier[12] through visual inspection and spectral analysis by having "flat"

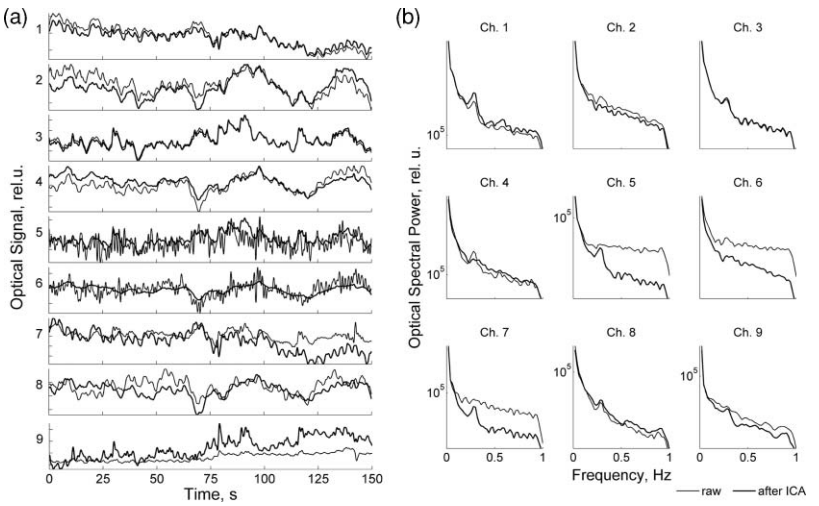

Fig. 6 (a) Raw optical signals (thin line) and the same signals after ICA-based artifact removal (thick line). (b) The corresponding power spectra of channels shown in (a).

spectra typical for white noise. Those ICA components were then excluded during restoration of the signal. As a result, optical signals became significantly less corrupted by noise and physiological rhythms could be seen even in originally "noisy" channels [see, for example, channels 5 and 7 in Fig. 6(b), where the remaining respiratory spectral peak at 0.25 Hz can be clearly seen after noise removal]. This illustrates the effectiveness of ICA in removing artifacts and noise generated in the superficial layers and improving signal-to-noise ratio of optical recordings. The restored signal was then used to calculate event-related responses as well as signal correlations.

3.2 *Optical Hemodynamic Signal: Amplitude Analysis*

An example of typical raw optical signals (after ICA-based denoising procedure) during quiescent periods and cognitive task are shown in Fig. 7. Cognitive tasks typically evoked a transient increase in oxygenated hemoglobin (ΔHbO = 0.5–2 μM) and a corresponding reduction in deoxygenated hemoglobin (ΔHb = 0.2–0.5 μM) (Fig. 7). The task-related response started within a few seconds after the beginning of the task and reached a peak at 10 s. After that time, the response was gradually decreasing toward the baseline but remained elevated (or reduced for Hb) over the whole period of task performance (Fig. 7).

The group average amplitude responses and the results of their statistical analysis are shown in Fig. 8. Scalp maps of group average responses obtained through image reconstruction and superimposed on a standard head template are presented in Fig. 2. The data clearly show a spatial pattern of task-related activation bilaterally within the inferior and the middle frontal gyri with a strong dominance of the right hemisphere (Fig. 8). The HbO response (an increase in concentration) appeared to have a greater subject-to-subject variation compared to the Hb response (a decrease in concentration). As a result, the average amplitudes of the HbO response were significantly different from baseline levels (assumed to be zero) only in the right hemisphere while the average amplitudes of the Hb response were significantly lower than the baseline level in both hemispheres and the level of significance was higher compared to the HbO response (Fig. 8). Although both HbO and Hb amplitude responses were greater in the right hemisphere, these hemispheric differences did not reach significance levels due to a relatively large variability between subjects.

3.3 *Optical Hemodynamic Signal: Functional Connectivity Analysis*

Functional connectivity based on interchannel correlation between hemodynamic responses showed clear changes related to the cognitive task while the baseline levels of connectivity were similar in both passive states [eyes closed and eyes open; Fig. 3(a)]. First, we compared task-related changes in unilateral functional connectivity between the IFG and the MFG to the baseline levels of connectivity during passive states. In

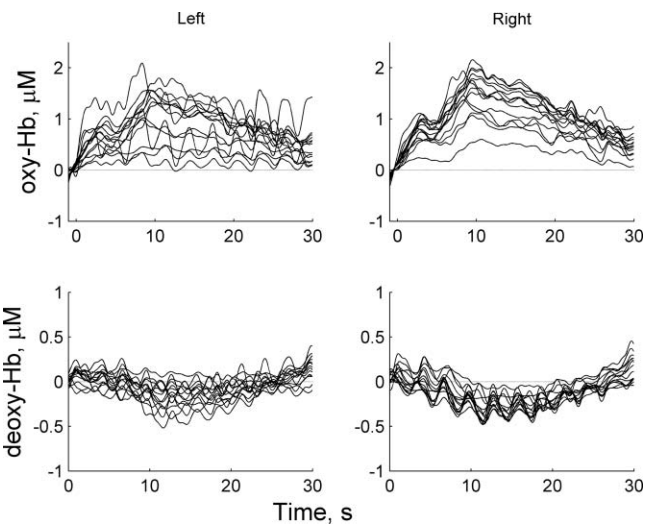

Fig. 7 A representative example of hemodynamic signals from one subject during the cognitive task for oxygenated (HbO, top) and deoxygenated (Hb, bottom) hemoglobin. Onset of the task is marked by $t = 0$. Note a smaller amplitude scale for Hb responses.

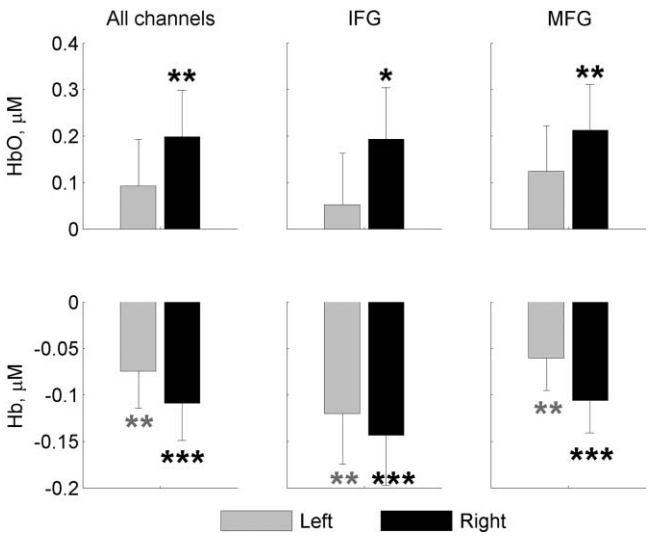

Fig. 8 Group average hemodynamic amplitude responses. Changes in concentrations of HbO and Hb are averaged over a 30-s time period of the task and compared to baseline (1-s time period immediately preceding the onset of the task) for the left and right hemispheres. IFG and MFG are the inferior and the middle frontal gyrus, respectively. Significant changes are indicated by asterisks; $p < 0.05$ (*), $p < 0.01$ (**), and $p < 0.001$ (***).

both hemispheres, functional connectivity increased during task performance, but these increases were significant only in the right hemisphere [$p < 0.05$ for the increase in correlation of HbO activity and $p < 0.01$ for the increase in correlation of Hb activity; Fig. 3(a), black asterisks]. Second, we compared task-related increases in unilateral connectivity in the left hemisphere versus the right hemisphere. For both forms of hemoglobin, an increase in connectivity was significantly greater in the right hemisphere [$p < 0.05$ for HbO and $p < 0.001$ for Hb; Fig. 3(a), gray asterisks]. Thus, the data on unilateral functional connectivity show the dominance of the right hemisphere during the object detection task. The corresponding spatial maps of connectivity are presented in Fig. 3(b), where the dominance of the right hemisphere is clearly seen. Here, each IFG/MFG voxel shows an average correlation of activity of that voxel with all MFG/IFG voxels within the same hemisphere thus representing unilateral connectivity within the region of interest (prefrontal cortex).

Third, we measured bilateral connectivity, that is, between the homologous areas in the left and right hemispheres. Baseline level of bilateral connectivity appeared to be relatively high (for HbO) and did not change during task performance (see top half of Fig. 9). The only significant increase in bilateral connectivity was observed for Hb in the middle frontal gyrus (see bottom half of Fig. 9). Thus, task-related changes in bilateral connectivity (i.e., across hemispheres) were much less pronounced compared to the changes in unilateral (specifically, right-hemispheric) connectivity.

3.4 *EEG Data*

Here we present only a small selection of the EEG data in order to compare them to the hemodynamic response. To demonstrate lateralization of the brain response during object recognition, we present scalp maps calculated for phase-locked high β–low γ activity (20–40 Hz). Those scalp maps were calculated at every time point within an interval from 0.05 to 0.4 s after stimulus onset, and Fig. 4 represents maps at time points where the corresponding differential electrophysiological parameter attained the maximal value (i.e., β–γ band activity calculated as the difference between the target- and nontarget-related responses). High-frequency response (20–40 Hz) showed two major loci of activation during this cognitive task, one in the occipital areas and another in the frontal areas. This electrophysiological response developed earliest (0.11 s after stimulus onset) and showed a significant right-hemispheric lateralization for both the occipital and the prefrontal sources of activity especially

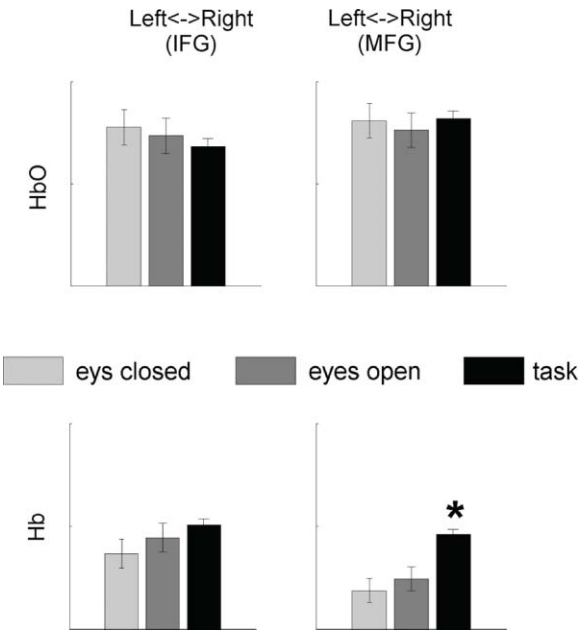

Fig. 9 Group average values of bilateral (interhemispheric) functional connectivity during resting periods and during task performance. IFG and MFG are the inferior and the middle frontal gyrus, respectively. Significant changes (compared to the resting periods) are indicated by asterisk ($p < 0.05$).

prominent at $t = 150$ ms when the response was at its peak (Fig. 4).

4 Discussion

The present study used near-infrared spectroscopy to investigate the involvement of prefrontal cortex in rapid detection of complex objects. The major goal was to demonstrate the capability of optical imaging to provide useful information about spatial localization of cognitive functions specifically, to demonstrate hemispheric lateralization (if any) of prefrontal activation during early visual processing. Our experimental paradigm was a combination of an event-related design commonly used in ERP studies and a block design commonly used in the studies of brain hemodynamic activity. Thus, we presented 12 stimulation blocks each consisting of 100 trials (with targets and nontargets presented randomly) varying in duration from 900 to 1700 ms. This design allowed us to measure electrophysiological parameters (such as conventional ERP and event-related time-frequency spectrograms) as well as a block-averaged hemodynamic response related to task performance. Another distinctive feature of the study was the assessment of functional connectivity within the prefrontal cortex during the task, which was based on correlation of optical signals within and between selected groups of channels. in this way, we were able to measure connectivity in each hemisphere between IFG and MFG (unilateral connectivity) as well as connectivity between the homologous structures of both hemispheres (bilateral connectivity). Although functional connectivity is commonly studied using fMRI or PET technologies, we are aware of only a few studies where functional connectivity has been measured by NIRS.[19–21] Thus, our study makes an important step extending the range of possible applications of NIRS technology.

In a previous study,[12] we applied ICA with the goal to remove artifactual components from the optical signal (mostly related to the contribution of superficial layers, such as scalp and skull) and thus to increase the signal-to-noise ratio of the fast optical signal presumably related to neuronal activity. We have demonstrated that the SNR could be significantly increased using ICA, and the fast signal could be recorded in the majority of our subjects.[12] The ICA has been successfully applied for electrophysiological signals such as EEG and MEG in numerous applications, but there are only a few studies where the ICA has been applied to the optical data. Thus, a recent study has successfully employed ICA to remove the skin blood flow artifact from functional near-infrared spectroscopic imaging data.[22] The ICA method has also been used to improve the SNR in optical imaging of intrinsic signals,[23,24] and we are aware of only one study where ICA was applied to detect fast optical signal in frequency-domain measurements.[25] In the present study, we have applied ICA to the "slow" optical signal, that is, to the signal sensitive to hemodynamic activity of the brain. Our current results confirm the efficacy of ICA as a powerful denoising tool applicable for the analysis of hemodynamic activity recorded optically.

During task performance, we observed a clear hemodynamic response in the prefrontal areas of the cortex. This response, as commonly found in optical measurements during various functional tasks,[26–29] included both an increase in [HbO] and a decrease in [Hb]. Most importantly, this response was greater in the right hemisphere (Fig. 8) although the difference between the right versus left hemisphere did not reach significance in the amplitude response due to a relatively large individual variations. An interesting aspect of the task-related hemodynamic response was an increase in functional connectivity as measured by pairwise correlations within the multichannel optical data. Both [HbO] and [Hb] responses demonstrated increases in signal correlations during cognitive task as compared to the baseline level of correlation observed during passive states with eyes open and eyes closed (Fig. 3). Most revealing in terms of hemispheric lateralization, those increases were significantly greater than baseline correlations in the right hemisphere only. Also, correlations in both [HbO] and [Hb] signals were significantly greater in the right versus left hemisphere (Fig. 3). Thus, both amplitude and correlation measures of hemodynamic responses during object recognition task point to the primary involvement of the right hemisphere in this process. Previously, NIRS has been successfully used for language lateralization.[30] Our results also demonstrate the usefulness of NIRS in the studies of lateralization of cognitive functions.

Previous findings have shown that target and nontarget ERPs during the Animal–No-Animal task start to diverge around 150 ms after stimulus onset and the differential ERP activity (i.e., the difference between target- and nontarget-related ERP) reaches a peak at 200 ms. Also, the ERP is larger in amplitude for nontargets (more positive in the occipital and more negative in the frontal cortex). As a result, the differential ERP (target > nontarget) has positive polarity over frontal and central areas and negative polarity over temporal and occipital regions. We are not aware of any studies on time-frequency analysis of brain electrical activity during the animal–no-animal paradigm. Our results show that the early brain response during animal–no-animal task contains a burst of phase-locked high-frequency activity within the high β and low γ range (20–40 Hz) and this burst appears at 110 ms, which is *earlier* than the divergence in the ERP (Fig. 4). Another interesting finding is that high-frequency responses were greater in the right hemisphere during perception of targets. Thus, our data provide converging evidence based on the optical hemodynamic response as well as the β–γ evoked electrical activity that rapid recognition of complex objects involves early activation of the prefrontal cortex preferentially in the right hemisphere.

Also of note is the result that hemispheric lateralization demonstrated in this study was statistically significant for functional connectivity only. The hemispheric differences in the amplitude of the hemodynamic response did not reach significance due to a relatively large inter-individual variability. We therefore suggest that the correlation of optical signals provides a measure complimentary to (and in some cases even more sensitive than) the measure of brain activation based on signal amplitude.

The intrinsic ambiguity of a Go-NoGo task is that, in addition to processing of sensory information and generating a "recognition event," the task requires a specific motor act (button pressing) in response to target objects only. This question was addressed by Herrmann et al. who used optical imaging during a similar Go-NoGo task.[31] These authors compared brain activation during the Go-NoGo task (the "NoGo" condition when response is produced or inhibited to targets or nontargets, respectively) to the "Go" condition (control) requiring button

pressing in response to all stimuli. For such a differential response, they found greater activation of the inferior frontal cortex bilaterally which they attributed to the response inhibition process. In our experiments, we compared Go-NoGo task-related activation to the passive states ("no task" condition) and did not attempt to distinguish between recognition of targets versus nontargets, both of which were present within the blocks of serial picture presentations. Although we cannot ascertain whether the observed brain activation is due to the "perception" of a target or response inhibition, the existing evidence is that both perceptual analysis and response inhibition involve predominantly the right hemisphere. Neuroimaging studies specifically focusing on response inhibition have demonstrated the right hemispheric lateralization of the response inhibition process.[32,33] An important role of the right hemisphere in the perceptual analysis and recognition of faces and objects has been also demonstrated in neuroimaging, electrophysiological, lesion, and behavioral studies.[34–37] Thus, our data are consistent with the data obtained with other imaging modalities and provide further evidence for the important role of the frontal cortex in object recognition and decision-making processes.

Visual recognition of complex objects is surprisingly fast (150–200 ms), and some models suggest exclusively a bottom-up process through the ventral visual processing pathway, starting in the primary visual cortex and culminating in the activity of high-level feature neurons (image detectors) in the inferior temporal cortex (IT). However, there is growing evidence on possible involvement of top-down processes from the prefrontal cortex (PFC) presumably "guiding" target feature selection and evaluation. It has been suggested that the PFC receives partial and incomplete information about the visual object (presumably, low spatial frequency information) early and directly from the primary visual cortex through the dorsal magnocellular pathway. This information is used to generate "initial guesses" about the object which are then conveyed as top-down influences and help to guide final recognition occurring within the IT.[38,39] As the MEG and fMRI data show, during object recognition the activation in the right PFC happens indeed very early (∼100 ms) and it is likely to reflect activation of the dorsal pathway leading to the early activation of the left orbitofrontal cortex, which is presumably a primary source of top-down control in visual object recognition.[39] The chain of events during the early phases of visual processing thus involves the propagation of activity through a number of structures in the PFC starting with the activation of the right frontal eye field (see the supplementary Fig. 8 in Ref. 39) and ending in the orbitofrontal cortex[39]). The hemodynamic response observed in our experiments is therefore likely to reflect a spatiotemporal summation of all these events leading to a relatively widespread activity observed in the frontal cortex and an increased correlation between the middle and the inferior frontal cortices.

5 Conclusions

Our results demonstrate that functional connectivity can be measured by optical methods with high temporal resolution detecting transient changes in functional connectivity during rapid object recognition. The results provide a supportive evidence for the model of top-down influences from the prefrontal cortex onto the ascending visual processing route. Correlation analysis of the optical BOLD signals may provide a sensitive measure of both local and long-distance functional connectivity during cognitive tasks, which may be used for lateralization and cortical mapping of brain processes in a variety of clinical applications. Overall, these data demonstrate the usefulness of optical imaging in the fast event-related paradigms in providing further information not only on spatial localization but also on interregional interactions during cognitive processes.

Acknowledgments

This work was supported by the NIH (Grant No. R01EB006589 to A.M.), DARPA (Grant No. HB1582–05-C-0045 to J.V.), and The Nancy Lurie Marks Family Foundation.

References

1. K. J. Friston, C. D. Frith, P. F. Liddle, and R. S. Frackowiak, "Functional connectivity: the principal-component analysis of large (PET) data sets," *J. Cereb. Blood Flow Metab.* **13**(1), 5–14 (1993).
2. S. Thorpe, D. Fize, and C. Marlot, "Speed of processing in the human visual system," *Nature* **381**(6582), 520–522 (1996).
3. A. Pfefferbaum, J. M. Ford, B. J. Weller, and B. S. Kopell, "ERPs to response production and inhibition," *Electroencephalogr. Clin. Neurophysiol.* **60**(5), 423–4234 (1985).
4. M. Codispoti, V. Ferrari, M. Junghofer, and H. T. Schupp, "The categorization of natural scenes: brain attention networks revealed by dense sensor ERPs," *Neuroimage* **32**(2), 583–591 (2006).
5. A. Kok, "Effects of degradation of visual stimulation on components of the event-related potential (ERP) in go/nogo reaction tasks," *Biol. Psychol.* **23**(1), 21–38 (1986).
6. M. Eimer, "Effects of attention and stimulus probability on ERPs in a Go/Nogo task," *Biol. Psychol.* **35**(2). 123–138 (1993).
7. A. Delorme, G. Richard, and M. Fabre-Thorpe, "Ultra-rapid categorisation of natural scenes does not rely on colour cues: a study in monkeys and humans," *Vision Res.* **40**(16), 2187–2200 (2000).
8. M. Fabre-Thorpe, A. Delorme, C. Marlot, and S. Thorpe, "A limit to the speed of processing in ultra-rapid visual categorization of novel natural scenes," *J. Cogn. Neurosci.* **13**(2), 171–180 (2001).
9. J. S. Johnson and B. A. Olshausen, "Timecourse of neural signatures of object recognition," *J. Vis.* **3**(7), 499–512 (2003).
10. A. Antal, S. Keri, G. Kovacs, Z. Janka, and G. Benedek, "Early and late components of visual categorization: an event-related potential study," *Brain Res. Cogn. Brain Res.* **9**(1), 117–119 (2000).
11. A. Delorme, G. A. Rousselet, M. J. Mace, and M. Fabre-Thorpe, "Interaction of top-down and bottom-up processing in the fast visual analysis of natural scenes," *Brain Res. Cogn. Brain Res.* **19**(2), 103–113 (2004).
12. A. V. Medvedev, J. Kainerstorfer, S. V. Borisov, R. L. Barbour, and J. VanMeter, "Event-related fast optical signal in a rapid object recognition task: improving detection by the independent component analysis," *Brain Res.* **1236**, 145–158 (2008).
13. D. Kim, S. W. Kim, E. Y. Joo, W. S. Tae, S. J. Choi, and S. B. Hong, "Cortical localization of scalp electrodes on three-dimensional brain surface using frameless stereotactic image guidance system," *Neurol. Asia* **12**(Suppl. 1), 84 (2007).
14. Y. Hochberg and A. C. Tamhane, *Multiple Comparison Procedures*, Wiley, Hoboken, NJ (1987).
15. R. Oostenveld, P. Fries, and O. Jensen, *Fieldtrip toolbox*, http://www.ru.nl/fcdonders/fieldtrip (2007).
16. R. Galambos, "A comparison of certain gamma band (40 Hz) brain rhythms in cat and man," in *Induced Rhythms in the Brain*, E. Basar and T. H. Bullock, Eds., pp. 201–216 Birkhauser, Boston (1992).
17. C. R. Genovese, N. A. Lazar, and T. Nichols, "Thresholding of statistical maps in functional neuroimaging using the false discovery rate," *Neuroimage* **15**(4), 870–878 (2002).
18. A. Delorme and S. Makeig, "EEGLAB: an open source toolbox for analysis of single-trial EEG dynamics including independent component analysis," *J. Neurosci. Methods* **134**(1), 9–21 (2004).

19. E. Rykhlevskaia, M. Fabiani, and G. Gratton, "Lagged covariance structure models for studying functional connectivity in the brain," *Neuroimage* **30**(4), 1203–1218 (2006).
20. B. R. White, A. Z. Snyder, A. L. Cohen, S. E. Petersen, M. E. Raichle, B. L. Schlaggar, and J. P. Culver, "Resting-state functional connectivity in the human brain revealed with diffuse optical tomography," *Neuroimage* **47**(1), 148–156 (2009).
21. Y. J. Zhang, C. M. Lu, B. B. Biswal, Y. F. Zang, D. L. Peng, and C. Z. Zhu, "Detecting resting-state functional connectivity in the language system using functional near-infrared spectroscopy," *J. Biomed. Opt.* **15**(4), 047003 (2010).
22. S. Kohno, I. Miyai, A. Seiyama, I. Oda, A. Ishikawa, S. Tsuneishi, T. Amita, and K. Shimizu, "Removal of the skin blood flow artifact in functional near-infrared spectroscopic imaging data through independent component analysis," *J. Biomed. Opt.* **12**(6), 062111 (2007).
23. I. Schiessl, W. Wang, and N. McLoughlin, "Independent components of the haemodynamic response in intrinsic optical imaging," *Neuroimage* **39**(2), 634–646 (2008).
24. S. C. Chen, Y. T. Wong, L. E. Hallum, N. B. Dommel, S. L. Cloherty, J. W. Morley, G. J. Suaning, and N. H. Lovell, "Optical imaging of electrically evoked visual signals in cats: II. ICA "Harmonic Filtering" Noise Reduction," in *Conf. Proc. IEEE Eng. Med. Biol. Soc.* Vol. 1, pp. 3380–3383 (2007).
25. G. Morren, U. Wolf, P. Lemmerling, M. Wolf, J. H. Choi, E. Gratton, L. De Lathauwer, and S. Van Huffel, "Detection of fast neuronal signals in the motor cortex from functional near infrared spectroscopy measurements using independent component analysis," *Med. Biol. Eng. Comput.* **42**(1), 92–99 (2004).
26. M. A. Franceschini, S. Fantini, J. H. Thompson, J. P. Culver, and D. A. Boas, "Hemodynamic evoked response of the sensorimotor cortex measured noninvasively with near-infrared optical imaging," *Psychophysiology* **40**(4), 548–560 (2003).
27. M. A. Franceschini and D. A. Boas, "Noninvasive measurement of neuronal activity with near-infrared optical imaging," *Neuroimage* **21**(1), 372–386 (2004).
28. V. Toronov, M. A. Franceschini, M. Filiaci, S. Fantini, M. Wolf, A. Michalos, and E. Gratton, "Near-infrared study of fluctuations in cerebral hemodynamics during rest and motor stimulation: temporal analysis and spatial mapping," *Med. Phys.* **27**(4), 801–815 (2000).
29. V. Toronov, A. Webb, J. H. Choi, M. Wolf, A. Michalos, E. Gratton, and D. Hueber, "Investigation of human brain hemodynamics by simultaneous near-infrared spectroscopy and functional magnetic resonance imaging," *Med. Phys.* **28**(4), 521–527 (2001).
30. A. Gallagher, M. Theriault, E. Maclin, K. Low, G. Gratton, M. Fabiani, L. Gagnon, K. Valois, I. Rouleau, H. C. Sauerwein, L. Carmant, D. K. Nguyen, A. Lortie, F. Lepore, R. Beland, and M. Lassonde, "Near-infrared spectroscopy as an alternative to the Wada test for language mapping in children, adults and special populations," *Epileptic Disord.* **9**(3), 241–255 (2007).
31. M. J. Herrmann, A. C. Ehlis, A. Wagener, C. P. Jacob, and A. J. Fallgatter, "Near-infrared optical topography to assess activation of the parietal cortex during a visuo-spatial task," *Neuropsychologia* **43**(12), 1713–1720 (2005).
32. R. Kawashima, K. Satoh, H. Itoh, S. Ono, S. Furumoto, R. Gotoh, M. Koyama, S. Yoshioka, T. Takahashi, K. Takahashi, T. Yanagisawa, and H. Fukuda, "Functional anatomy of GO/NO-GO discrimination and response selection—a PET study in man," *Brain Res.* **728**(1), 79–89 (1996).
33. H. Garavan, T. J. Ross, and E. A. Stein, "Right hemispheric dominance of inhibitory control: an event-related functional MRI study," *Proc. Natl. Acad. Sci. U.S.A.* **96**(14), 8301–8306 (1999).
34. N. Kanwisher, J. McDermott, and M. M. Chun, "The fusiform face area: a module in human extrastriate cortex specialized for face perception," *J. Neurosci.* **17**(11), 4302–4311 (1997).
35. A. Low, S. Bentin, B. Rockstroh, Y. Silberman, A. Gomolla, R. Cohen, and T. Elbert, "Semantic categorization in the human brain: spatiotemporal dynamics revealed by magnetoencephalography," *Psych. Sci.* **14**(4), 367–372 (2003).
36. G. Yovel and N. Kanwisher, "Face perception: domain specific, not process specific," *Neuron* **44**(5), 889–898 (2004).
37. J. S. Simons, W. Koutstaal, S. Prince, A. D. Wagner, and D. L. Schacter, "Neural mechanisms of visual object priming: evidence for perceptual and semantic distinctions in fusiform cortex," *Neuroimage* **19**(3), 613–626 (2003).
38. M. Bar, "A cortical mechanism for triggering top-down facilitation in visual object recognition," *J. Cogn. Neurosci.* **15**(4), 600–609 (2003).
39. M. Bar, K. S. Kassam, A. S. Ghuman, J. Boshyan, A. M. Schmid, A. M. Dale, M. S. Hamalainen, K. Marinkovic, D. L. Schacter, B. R. Rosen, and E. Halgren, "Top-down facilitation of visual recognition," *Proc. Natl. Acad. Sci. U.S.A.* **103**(2), 449–454 (2006).